. Printed in U.S.A.

68-GT-26

an ASME publication

$1.50 PER COPY
75¢ TO ASME MEMBERS

DIGATEC
(Digital Gas Turbine Engine Control)

J. E. BAYATI

Research Specialist, Advanced Control Systems, Autonetics Division, North American Rockwell Corp., Anaheim, Calif.

R. M. FRAZZINI

Senior Research Engineer, Advanced Control Systems, Autonetics Division, North American Rockwell Corp., Anaheim, Calif.

The basic operating principles of an electronic digital computer gas turbine engine control system are presented. Closed loop turbine discharge temperature and speed controls have been implemented; their feasibility was demonstrated through hybrid digital/analog simulation and actual tests of a GE J85 turbojet engine through the start mode to maximum afterburner. Control mode description and results of the analysis and experimental runs are given in this paper.

Contributed by the Gas Turbine Division of The American Society of Mechanical Engineers for presentation at the Gas Turbine Conference & Products Show, Washington, D.C., March 17-21, 1968. Manuscript received at ASME Headquarters, December 28, 1967.

Copies will be available until January 1, 1969.

DIGATEC
(Digital Gas Turbine Engine Control)

J. E. BAYATI **R. M. FRAZZINI**

NOMENCLATURE

A_8 = exhaust nozzle area
A_{8_c} = exhaust nozzle area command
A_{8_d} = exhaust nozzle area demand
A_c^1 = required steady state exhaust nozzle area
ΔA_L = acceleration loop contribution to exhaust nozzle area command
ΔA^L = limit on acceleration loop contribution to exhaust nozzle area command
$\Delta A_{8_{a/b}}$ = bias on exhaust area due to a/b command
K = speed control gain
K_1 = integral gain
$K_{\dot{N}}$ = engine rotor acceleration gain
$K_{\dot{N}}$ = rate of change of engine speed with respect to fuel flow
N_e = engine speed
N_c = engine speed command (function of power level position)
N_{LIM} = overspeed limit
$N_e/\sqrt{\theta}$ = corrected speed
$\dot{N}_e$ = engine rotor acceleration
ΔN_e = speed error $N_c - N_e$
ΔN_1 = value the speed error must exceed before acceleration path of exhaust nozzle loop is coupled
T = temperature, deg R
P = pressure, psi
ΔN_L = limited speed error
ΔN^L = error limit
$\Sigma \Delta N_e$ = digital integral of speed error
$(K_1 \Sigma \Delta N_e)^L$ = integral error limit
$\Sigma(\Delta N_L - K_{\dot{N}} \dot{N}_e)$ = digital integration of engine acceleration error
$\left[K_1 \Sigma(\Delta N_L - K_{\dot{N}} \dot{N}_e)\right]^L$ = integral acceleration error limit
P_2 = compressor inlet pressure
P_3 = compressor discharge pressure
P_{3REF} = value of P_3 at instant ΔN_e exceeds ΔN_1
P_5 = turbine discharge pressure
P_3/P_2 = compressor pressure ratio
$P_3/P_2|_0$ = steady state compressor pressure ratio
$\frac{\partial P_3/P_2}{\partial W_f}$ = rate of change of pressure ratio with respect to fuel flow
W_f = engine fuel flow
W_{f_c} = engine fuel flow command
W_{f_d} = speed control loop fuel requirement
W_{f_o} = engine steady-state fuel flow
W'_{f_d} = afterburner fuel flow demand
$\frac{W_f}{\delta\sqrt{\theta}}$ = corrected fuel flow
$W_f|_{a/b}$ = afterburner overtemperature trim
$W_{fa/bc}$ = afterburner fuel flow command
W_f/P_3 = fuel flow per unit compressor discharge pressure
$W_f/P_{3\ d}$ = W_f/P_3 control demand
$W_f/P_3|_{Bias}$ = control bias on W_f/P_3
$W_f/P_3|_{acc}$ = acceleration limit on W_f/P_3
$W_f/P_3|_{Min}$ = minimum limit on W_f/P_3
$W_f/P_3|_e$ = required change in W_f/P_3 Bias
$W_f/P_3|_{a/b}$ = afterburner fuel flow per unit compressor discharge pressure
a = throttle command (power lever position)
β_v = inlet guide vanes and bleed valve position
β_{v_c} = inlet guide vanes and bleed valves command
$\delta = P_2/14.7$
$\theta = T_2/519$
τ_e = engine rotor time constant
ω_c = metering valve minimum break frequency

Subscripts

0 - 8 = engine station locations
c = command
d = demand

INTRODUCTION

The increasing complexities and performance requirements of aircraft propulsion systems have put severe requirements on the presently accepted methods of control. Continuously optimized performance to achieve maximum range is becoming a necessity for the modern aircraft with its complex avionic and armament systems. In-flight monitoring, failure prediction, and failure correction by utilization of alternate control modes, as well as automatic preflight self test of the entire system, must become part of a total system management concept. These concepts, plus the need for increased engine performance by operation close to surge limits, and the resulting sensitivities to the inlet system and aircraft attitude and attitude rates, have stimulated creation of the "integrated" propulsion system concept.

The digital computer offers a tool with which an integrated propulsion system may be centrally organized. Rapid communication between subsystems, and accurate modeling of complex mathematical functions is a basic characteristic of a computer control system. The capability of the computer to handle a large number of input and output variables makes it ideal for application to the peripheral aspects of on-line optimization, performance monitoring and fail operational techniques, as well as direct propulsion system management.

This paper offers some typical control mode concepts studies at Autonetics during two engine test programs. These concepts were intentionally simplified to demonstrate the versatility of computer control. A combined analog/digital simulation was conducted to evaluate the performance of the selected control modes and define the initial gains and constants to be used in the test phase. It was understood that these values would probably change once the testing was initiated, due to the inability of a simplified simulation to accurately represent the actual engine.

Tests were run on a modified J85-1 and an afterburning J85-5. The hydromechanical controls were completely removed for all phases of the tests; the computer-to-engine interfacing was done with off the shelf sensors, metering valves, and electronics. Airborne type computers were used throughout the tests with excellent results.

Work is presently in progress on the more sophisticated concepts mentioned above, as well as hardware investigations on both electronic and mechanical devices. These studies, coupled with suitable testing, should provide a functional concept for advanced propulsion system management.

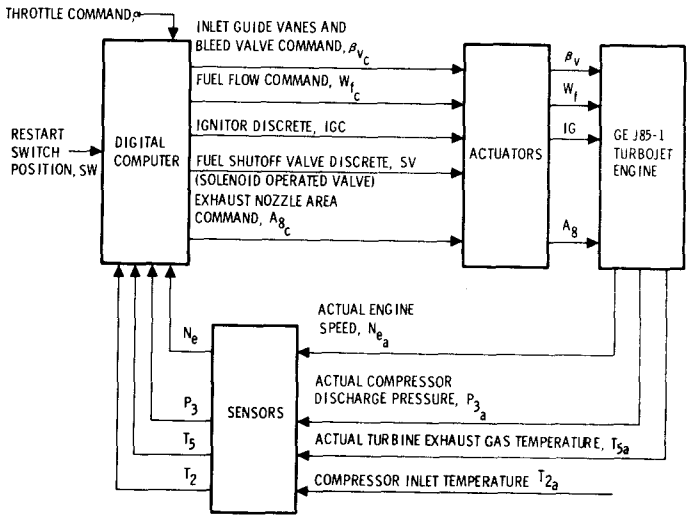

Fig.1 Engine control information flow diagram

Introduction

Consideration of the available J85-1 engine parameters, the available sensors and the control requirements narrowed the control modes that could logically be tested on the engine. The selected control modes were mechanized and evaluated through linear sample data techniques, as well as a hybrid analog/digital nonlinear real-time simulation study. A list of the equations used during the analysis and simulation phases is given in Appendix 1, and the results of the analysis and test phases are briefly described along with each of the subject control modes.

In addition to the closed loop control modes, several auxiliary functions such as start and shutdown sequences, open loop control of the compressor inlet guide vanes, and interstage bleed valves were performed. These functions were common to each control mode and are described in the following paragraphs.

Engine-Control Information Flow

The modified GE J85-1 turbojet engine independent parameters consisted of compressor inlet guide vanes, interstage bleed valves, exhaust nozzle area, and fuel flow. These parameters were manipulated as functions of external command (power lever), inlet conditions and engine state variables. Fig.1 represents the form of information exchange between the engine and the digital computer. This exchange, carried out through the actuators and sensors, allowed complete engine control through the digital computer from the start mode to military power.

The external command to the digital computer establishing the desired engine operating point was in the form of a voltage level which was set

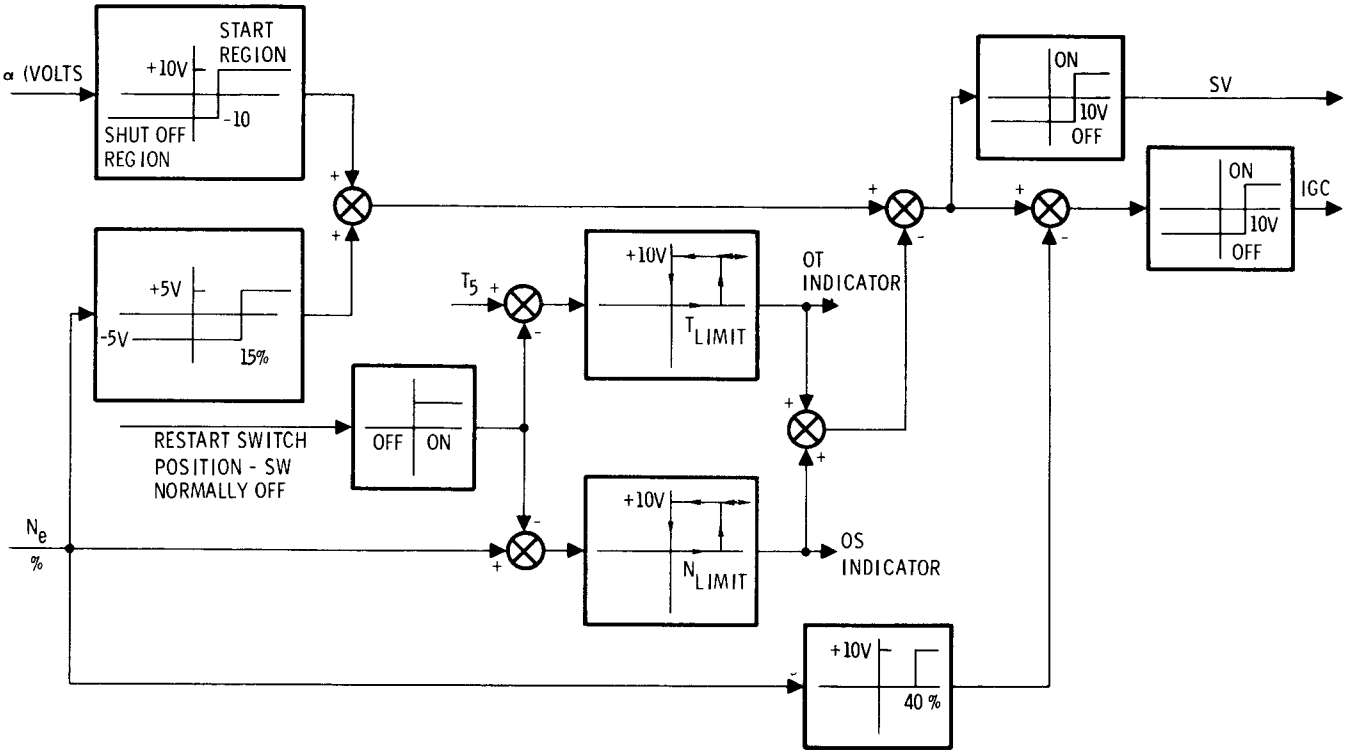

Fig.2 Engine start and shutdown sequence

through action of a throttle command lever (α). A switch was also provided to allow engine restart following overspeed and/or overtemperature shutdown.

The engine inlet condition was defined by the compressor inlet temperature, T_2, while the sensed engine parameters for the control modes studied were the engine rotor speed, N_e, and the compressor discharge pressure, P_3. Turbine discharge temperature, T_5, was used for overtemperature shutdown in the J85-1 control system, as well as temperature control in the J85-5 afterburner tests.

The digital computer output commands were main fuel flow, W_{f_c}, compressor inlet guide vanes and bleed valves position, β_{v_c}, exhaust area, A_{8C}, and fuel shutoff valve and ignition discretes. Afterburner fuel flow, $W_{f_{a/bc}}$, was added for the J85-5 tests.

Start and Shutdown Sequence for Test Installation

Start Sequence. The start sequence of events is shown in Fig.2. The start mode was initiated by placing the power lever above the shutoff region. As the engine windmilling speed exceeded 15 percent, discretes were issued to activate the ignitor and open the solenoid-operated fuel shutoff valve. The ignitor discrete was removed as soon as the rotor speed exceeded 40 percent, completing the start sequence. The engine speed stabilized at a level determined by the power lever position.

Shutdown Sequence. Shutdown was commanded by retarding power lever to within the shutoff region which issues a discrete from the computer closing the fuel shutoff valve. This valve was independent of the main fuel metering system. Emergency shutdown could be initiated as a result of an overspeed ($N_e > N_{Limit}$) or turbine exhaust gas overtemperature ($T_5 > T_{Limit}$) condition which would trigger the above computer discrete. Hysteresis was built into the overspeed and overtemperature indicator logic, which prevented initiation of a restart sequence when the engine speed or temperature returned to normal. The restart sequence could be initiated after the speed fell below 40 percent by activating the normally off restart switch which resets the applicable logic. At the time of initiation of emergency shutdown, a signal would be transmitted to indicate the cause of shutdown to the operator.

Compressor Inlet Guide Vanes and Interstage Bleed Valve Loop

A single actuator controlled the positions of the compressor inlet guide vanes and the interstage air bleed valves. The actuator command, β_{v_c}, was scheduled as a function of the engine

corrected speed, $N_e/\sqrt{\theta}$. During engine rotor acceleration, no attempt was made to provide a bias to unload the front stages of the compressor by opening the bleed valves since the valves were normally required to be wide open until high corrected speed was attained.

Exhaust Nozzle Area Control Loop

There are several approaches to the control of exhaust nozzle area. According to the method used to set the reference, the approach may be classified as one of two basic control concepts; i.e., the independent parameter input reference and the dependent parameter input reference.

General Concepts.

Independent Parameter Input Reference. With the exhaust nozzle area as the main control parameter the power lever schedules either the desired area or the turbine inlet or exhaust temperature. In the simplest case, the power lever positions the exhaust nozzle area which yields a very stable control. Utilizing either turbine temperatures, the power lever schedules the temperature demand. Closed loop control of this temperature is accomplished through exhaust nozzle area variation.

The disadvantage of scheduling the exhaust nozzle area as a function of power lever is the fact that the scheme does not allow for performance variations in engines, or that the desired area may vary with the ambient conditions. Scheduling the turbine temperature as a function of power lever, on the other hand, yields an optimized performance as compared to scheduling area. This method provides maximum performance independent of inlet conditions and, when combined with an afterburner system, will automatically compensate for the afterburner operation. Thus, no change in the basic control mode is required for afterburning.

Parameters scheduled as functions of power lever position suffer the common disadvantage of causing the controlled parameter, whether area or temperature, to go directly to the requested level upon a throttle burst. In many conditions, this is undesirable as it increases the acceleration time and degrades the surge margin.

It should be pointed out that the engine speed is assumed to be controlled in the above methods by modulation of fuel flow. It is possible, and may be desirable for certain applications, to control the engine speed by exhaust area modulation while controlling the turbine temperature by fuel flow modulation.

Dependent Parameter Input Reference. Any of the previous approaches, and some additional methods such as turbine pressure ratio control, can be related to engine speed rather than the power lever position to provide improved performance.

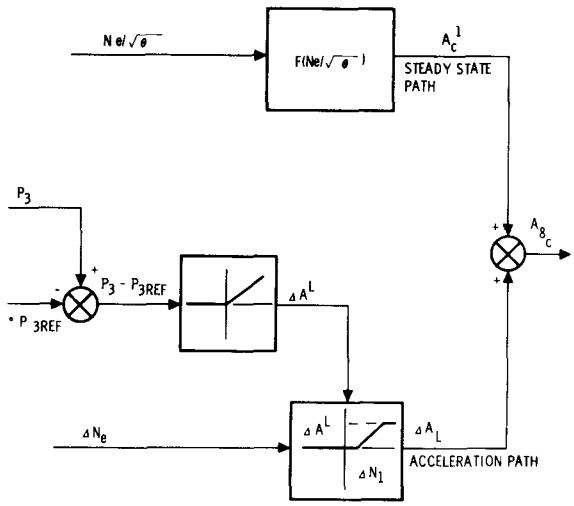

Fig.3 Exhaust nozzle area control system

For example, the speed and compressor inlet temperature could be used to set a reference for the desired turbine inlet temperature. The exhaust nozzle area is then modulated to attain the desired temperature. Similarly, the exhaust nozzle area could be scheduled as a function of a speed and compressor inlet temperature. Most of the disadvantages associated with the independent parameter method are eliminated, but at the risk of introducing stability problems.

Based on consideration of the above concepts and the available hardware, the exhaust nozzle area control of the test J85-1 engine was designed.

J85-1 Exhaust Nozzle Control. For the J85-1 turbojet engine, the exhaust nozzle area control scheme shown in Fig.3 was mechanized. This control system may be divided into steady-state and acceleration operating paths. The steady-state path is a function of the engine corrected speed, while the acceleration path is basically a function of speed error. This follows the dependent parameter scheme mentioned earlier.

An acceleration mode is said to exist when the engine speed error, ΔN_e, exceeds a positive constant, ΔN_1. The resulting control effort tends to increase the exhaust nozzle area during rotor acceleration. The desired increase in nozzle area, ΔA_8, is determined by multiplying the speed error in excess of ΔN_1 by a constant. ΔA_8 is then compared to a maximum limit, ΔA^L, and the smaller is added to the steady-state exhaust nozzle area command, A_c^1, to yield the total command, $A8_c$. At steady-state, A_c^1 and $A8_c$ are equivalent.

The maximum limit, ΔA^L, is a variable parameter whose value depends on the change in compressor discharge pressure from the point of initia-

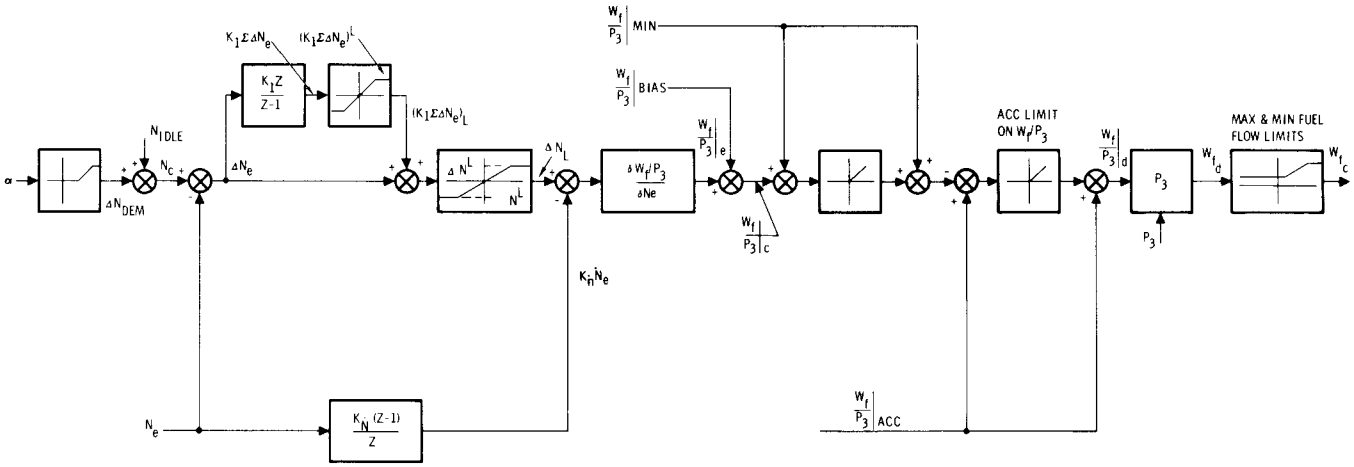

Fig.4 Proportional-integral speed control - Control Mode I

tion of the acceleration mode, ($\Delta P_3 = P_3 - P_{3REF}$). At the initiation of the acceleration mode, that is, when the engine speed error, ΔN_e, is sensed for the first time to be in excess of ΔN_1, the value of the compressor discharge pressure is picked up and stored in the computer as the pressure reference, P_{3REF}. This value remains constant through steady-state conditions following acceleration until the computer logic indicates that the engine speed error, ΔN_e, again exceeds ΔN_1. At this time, another acceleration mode is assumed to be in progress and the P_{3REF} initialization procedure is repeated.

The maximum limit, ΔA^L, is formed by multiplying the positive change in compressor discharge pressure following the initiation of an acceleration mode by a positive constant. If the change in pressure is negative, the limit is zero. The purpose of ΔA^L is to prevent the momentary reduction of engine thrust during acceleration due to rapid and unlimited opening of the exhaust nozzle area. Ideally, it is better to use the change in turbine discharge pressure, P_5, as an indication of thrust reduction. It was felt, however, that the low values of this pressure would result in a poor limiting scheme due to sensing and resolution problems. For applications where the exhaust nozzle area actuators are slow, a limiting scheme of this type is not necessary.

The nature of the acceleration path in the exhaust nozzle area control requires a priori knowledge of the steady-state engine speed error. In purely proportional speed control, this error is a function of engine speed, exhaust nozzle area, and inlet conditions. To decouple the acceleration loop during steady-state operation, the value of engine speed error, ΔN_e, must not exceed ΔN_1; consequently, ΔN_1 can no longer be made a constant. By placing an integral path in the speed control forward loop, the steady-state engine speed error, ΔN_e, is zero and a constant value for ΔN_1 can be effectively used.

Earlier, a distinction was made between the several available approaches to control the exhaust nozzle area. The flexibility of the digital concept was shown earlier to provide effective means to modify these methods with the aim of extracting improved steady-state and transient performance from the variable exhaust nozzle system. A second digital control concept, used during the J85-5 afterburner tests, will be described in a following section.

Engine Speed Control Modes

The engine rotor time constant and gain vary widely from idle to military power, from sea level to high altitudes, and for various vehicle Mach numbers. This variation of rotor dynamics requires a variable control gain for optimum dynamic performance at all flight conditions. Since changes in gain and time constant are essentially functions of engine air flow, compressor discharge pressure is an approximate measure by which the control gain may be varied.

The concept of using fuel flow per unit compressor discharge pressure, W_f/P_3, as a means to implement the control gain change has been accepted and proven to be effective. In this approach, the engine speed error generates a required W_f/P_3, which is then multiplied by the compressor discharge pressure, P_3, to yield the required engine fuel flow. The advantage of this approach extends further than the maintenance of a nearly constant system gain in that the resulting reduction in metered fuel flow upon compressor surge, due to the drop in compressor discharge pressure, is a built-in safety feature.

Two basic speed control modes were mechanized

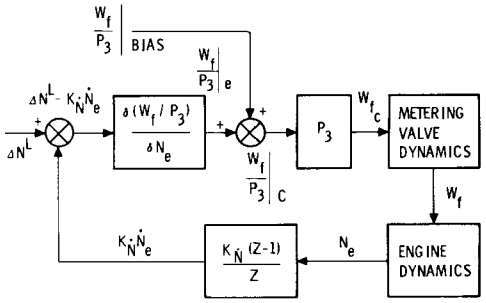

Fig.5 Acceleration loop - Control Mode I

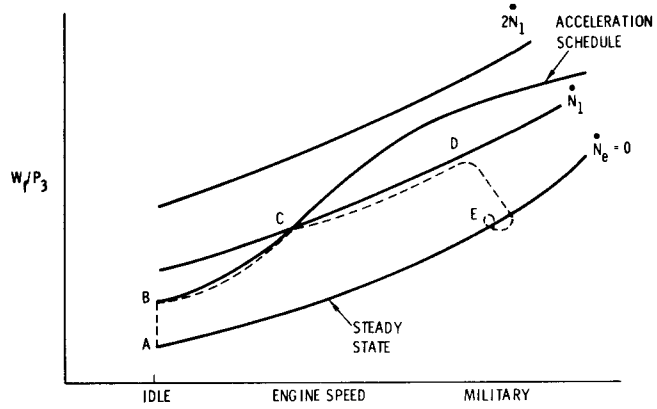

Fig.6 Example of acceleration limiting

around the W_f/P_3 concept, and were evaluated during the hybrid analog/digital real-time nonlinear simulation study and actual engine-control tests. Operation of these control modes is summarized in the following paragraphs.

Rate-Proportional-Integral Speed Control Mode (Control Mode I).

Control Mode Description. A simplified block diagram of this control mode is shown in Fig.4. The power lever position and the idle speed demand stored in computer memory established the final speed demand, N_c. The speed error and its digital integral are generated and added to form the parameter, $\Delta N_e + K_1 \Sigma \Delta N_e$. A signal proportional to the rotor acceleration, $\dot{N}_e$, is subtracted from this parameter and the result multiplied by the control gain to yield $W_f P_3|_e$, the required change in W_f/P_3 from the steady-state value, $W_f/P_3|_{Bias}$. The demand, $W_f/P_3|_c$, is then multiplied by the compressor discharge pressure, P_3, to arrive at the control fuel flow demand, W_{f_d}.

Integration in the digital computer is essentially a simple summing operation. It consists of the product of the sampling period and the accumulation of the value of the parameter at the start of the sampling period. Digital differentiation, on the other hand, is accomplished by dividing the change in the value of the parameter between two samples by the time period between the samples. This method was used to generate the rotor acceleration, $\dot{N}_e$, from the speed information. The success of this method was primarily due to the noise-free speed signal at the digital computer.

Several of the aforementioned parameters are limited prior to implementation of the control calculations. The control fuel flow demand, W_{f_d}, as well as the control demand, $W_f/P_3|_c$, is bounded by lower and upper limits. The lower limits prevent flameout during rapid deceleration while the upper limits prevent surge, overtemperature, and overpower. The maximum value of W_f/P_3 is generated as a function of engine speed and compressor inlet temperature.

The limit on the integral of speed error prevents computer overflow in addition to reduction of engine speed overshoot and undershoot during large transients.

The $W_f/P_3|_{Bias}$, employed to minimize the limits of the integral of speed error, is a function of speed demand and compressor inlet temperature. It is selected to yield approximately the steady state W_f/P_3.

Provisions are made in this control mechanization to limit the rotor acceleration, $\dot{N}_e$, when such a limit is desired. This is accomplished by selecting the proper error limit, ΔN^L. Engine rotor acceleration control has the potential of providing very accurate and repeatable transient characteristics. In application where minimum transient time is not a requirement and engine thrust matching is critical during transient as well as steady-state condition, as is the case in V/STOL application, this approach is desirable.

Consider the case where it is required to accelerate the engine speed from idle to military power at a specific inlet condition. At steady-state idle speed, the engine speed error is equivalent to zero due to the integral term in the control loop. Upon rapid advance of the power lever to the military position, a large speed error exists. As long as the sum of this error and its integral term is in excess of the error limit, ΔN^L, the value of the error limit, ΔN^L, is used in the control calculations. Under this condition, the error limit, ΔN^L, may be considered as the reference demand to the rotor acceleration, $\dot{N}_e$, thereby effectively decoupling rotor speed feedback. A simplified block diagram of the resulting acceleration control system is shown in Fig.5. The limits on W_f/P_3 and W_f are deleted in this block diagram for the sake of clarity.

In Fig.5, it is seen that the rotor acceleration control is a proportional loop. Because of engine characteristics, the rotor acceleration for any inlet condition and constant A_8 and $W_f/P_3|_{Bias}$

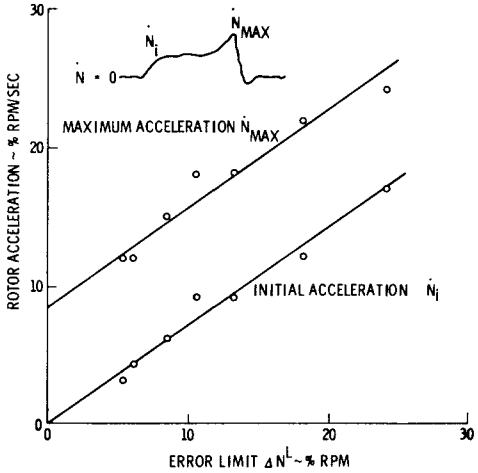

Fig.7 Effects of speed error limit on engine rotor acceleration during simulation of rapid transient - Control Mode I

depends on the error limit, ΔN^L, the acceleration gain, $K_{\dot{N}}$, the control gain, and the engine speed. For exact acceleration control, therefore, the error limit, ΔN^L, must be varied as a function of speed and inlet condition. For the purpose of the tests the error limit ΔN^L was maintained constant.

Fig.6 represents typical constant rotor acceleration lines and the surge and turbine inlet temperature limits in terms of W_f/P_3 versus engine speed for one inlet condition. As an example case, assume that the control parameters affecting the limit on the rotor acceleration are selected to yield a maximum rotor acceleration of $\dot{N}_1$. Upon rapid power lever advance from the idle to military position, the control demand, $W_f/P_3|_c$, as formed by the digital computer, will be limited by the acceleration schedule, B. The demand will continue to be limited by the acceleration schedule until the constant acceleration line, $\dot{N}_1$, intersects the acceleration schedule, C. At this point, the control demand will begin to track the constant acceleration line, $\dot{N}_1$, until the sum of the speed error and its integral term drops below the error limit, ΔN^L, D. At this point, the system reverts to a rate-proportional-integral control. The engine speed will settle at military power, E, following overshoot.

The overshoot is mainly the result of the integral term of the error which increased to its upper limit during the initial phase of the acceleration mode. It will not begin to drop below the limit until the military speed is exceeded.

Deceleration is accomplished in similar manner in that the lower error limit, $(-\Delta N^L)$, determines the deceleration level. All limits in the control system can be set independently of each other.

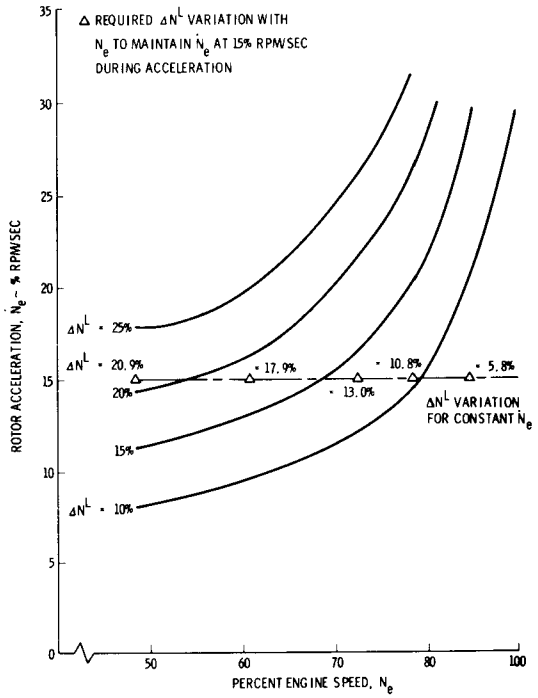

Fig.8 Engine rotor acceleration versus speed - Control Mode I

If minimum acceleration time in this control mode is desired, the error limit, ΔN^L, must be set sufficiently high such that the control demand, $W_f/P_3|_c$, during rapid acceleration always exceeds the acceleration schedule. This condition corresponds to demanding an acceleration level of $2\dot{N}_1$ in Fig.6.

Simulation Results. The following paragraphs present some of the results of the simulation study on Control Mode I for the modified J85-1. The engine was simulated on an analog computer, and the control concepts were programmed in the Autonetics VERDAN computer. This interface was a very close representation of the actual test setup in that the VERDAN was used in the test with the same program as that used on the simulation.

The rotor acceleration limiting loop was examined thoroughly. Rapid acceleration from idle to military speed was simulated for various values of the critical control parameters. The initial rotor acceleration level reached was found to be proportional to the speed error limit, ΔN^L. An increase in the error limit resulted in a proportional increase in the initial acceleration level, as shown in Fig.7. Also shown is the sharp increase in acceleration level occurring at high speeds. The difference between the initial and peak acceleration was nearly a constant equivalent to 8.5 percent military speed per second.

In order to maintain a constant rotor accel-

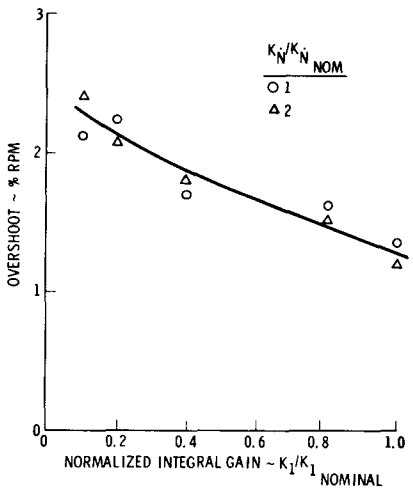

Fig.9 Effects of integral and acceleration gains on overshoot - Control Mode I

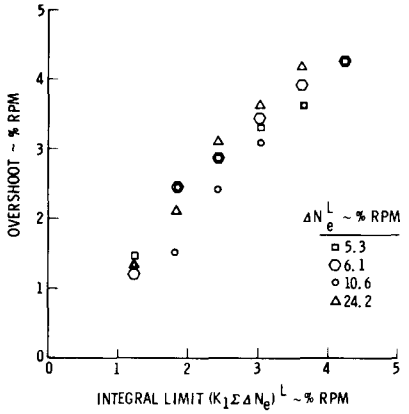

Fig.10 Effects of error integral limit and error limit on overshoot - Control Mode I

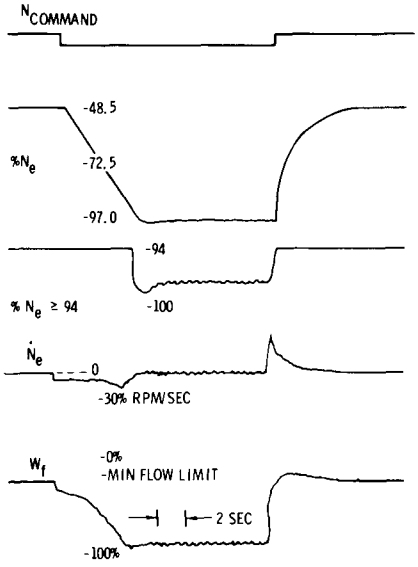

Fig.11 Simulated rapid transient with acceleration limiting control - Control Mode I

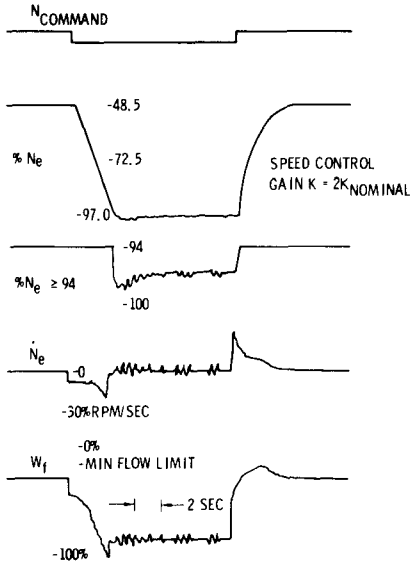

Fig.12 Simulated rapid transient with acceleration limiting control and excessive gain - Control Mode I

eration during large transients, it is necessary to vary the error limit, ΔN^L, as a function of engine speed. For a constant acceleration level of 15 percent of military speed per second, for example, the error limit, ΔN^L, must be varied as shown in Fig.8. For applications where wide variations in engine inlet condition are expected, the error limit must also be made sensitive to these conditions.

The effects of the integral error limit, $(K_I \Sigma \Delta N_e)L$, the error limit, ΔN^L, the acceleration gain, $K_{\dot{N}}$, and the integral gain, K_I, on the maximum observed overshoots during an idle to military speed rapid transient were determined. The overshoot appeared to be independent of the acceleration gain. This is illustrated by the data of Fig.9. Also shown in this figure is the effect of the integral gain variation, for constant integral error limit, $(K_I \Sigma \Delta N_e)^L$, on the overshoot. The magnitude of the overshoot appears to be inversely proportional to the integral gain. For the nominal engine parameters and the selected values for the control parameters, the maximum overshoot at military speed is estimated to be approximately 1.3 percent of military speed.

Fig.10 shows the effects of the integral error limit, $(K_I \Sigma \Delta N_e)^L$, upon the maximum observed overshoot, for a constant value of K_I, and various values of ΔN^L. The magnitude of the overshoot is independent of the error limit, ΔN^L, while it is directly proportional to the integral error limit.

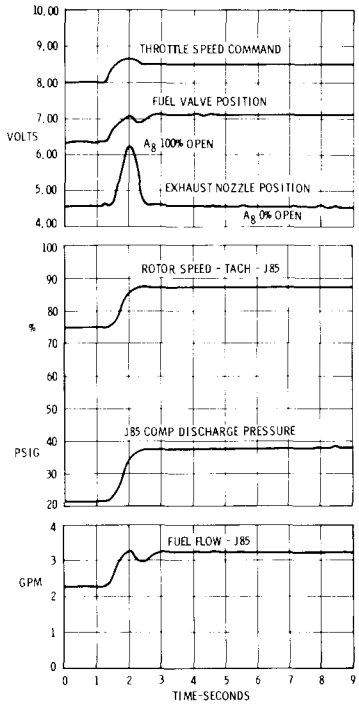

Fig.13 Rapid transient engine test from 75 to 87 percent speed - Control Mode I

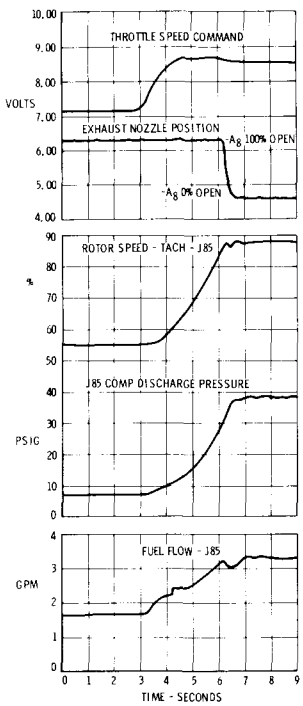

Fig.14 Rapid transient engine test from 55 to 88 percent speed - Control Mode I

Thus, any increase in the integral error limit results in a corresponding increase in the overshoot.

A typical time history profile of a simulated acceleration and deceleration mode of the system with the final selected value of the control parameters is shown in Fig.11.

The effects of the speed control gain, K, on system performance are shown in Fig.12. In this example, the gain is twice that of the case shown in Fig.11. In addition to making the system more oscillatory at high speed, the gain increased the acceleration level of the engine. This shift is due to the acceleration limiting control being a proportional loop.

Test Results. The time history profile of some of the system critical parameters are shown in Fig.13, for a rapid acceleration from 75 to 87 percent of military speed. The effect of the acceleration path on the nozzle area position is clearly shown in this figure. Following the application of command, the exhaust nozzle area went to 100 percent open then back to zero percent open as the final speed was approached, all in approximately 1 sec. The purpose of exhaust nozzle area modulation during transient is, as pointed out earlier, to increase available rotor acceleration. Fig.13 also indicates that the overshoot was negligible.

Fig.14 shows a rapid engine rotor acceleration from 55 to 88 percent of military speed. During this acceleration, the exhaust nozzle area remained partially open until the speed error approached zero. Here again, the overshoot is shown to be negligible.

In summary, system performance was very satisfactory in both acceleration, deceleration, and steady state. In particular, no measurable limit cycles and only moderate overshoots were observed during the entire engine test. The performance of the acceleration path in the exhaust nozzle area control loop appeared to be very satisfactory.

Integral Compensation on Engine Acceleration Error (Control Mode II).

Control Mode Description. The mechanization of the previous speed control mode had the capability of providing a soft limit on the rotor acceleration if desired. Control Mode II is a modification of this approach and is shown schematically in Fig.15. The W_f/P_3 limiting methods are not shown in the block diagram because of their similarity to those of Control Mode I.

In this control mode, a signal proportional to the rotor acceleration, $\dot{N}_e$, is subtracted from the limited engine speed error, ΔN_L. The resulting parameter and its limited integral are summed and multiplied by the control gain to form $W_f/P_3|_e$, the required change in $W_f/P_3|_{Bias}$. In this control mode the parameter $\Delta N_L - K_{\dot{N}} \dot{N}_e$, tends to be zero even during transients, provided the integral gain

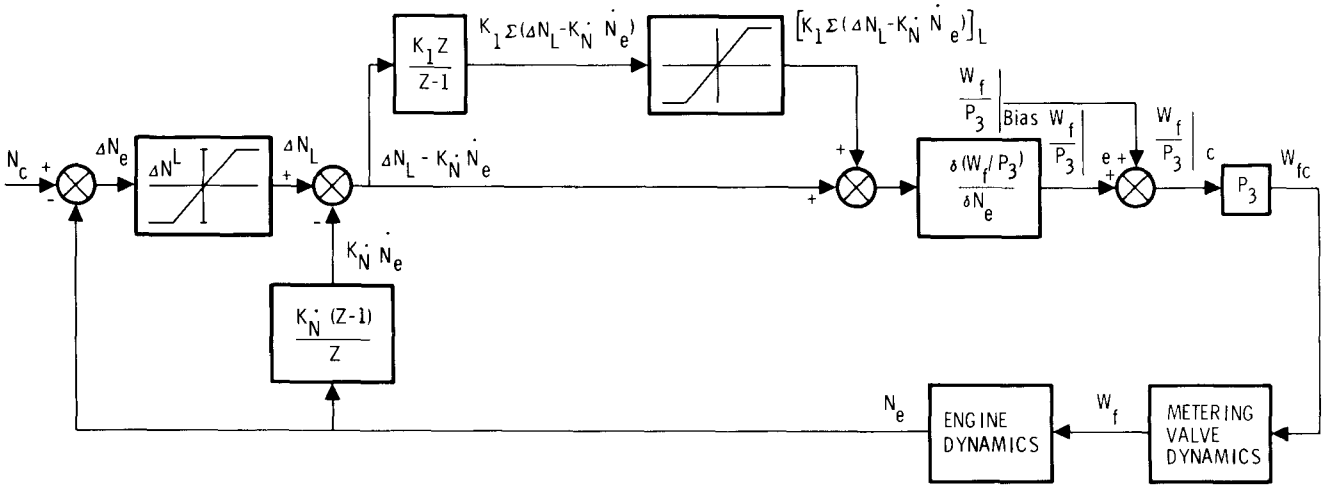

Fig.15 Integral compensation for engine acceleration error control - Control Mode II

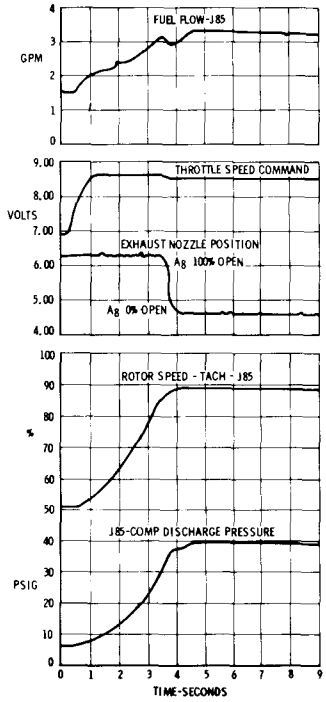

Fig.16 Rapid transient engine test from 51 to 88 percent speed - Control Mode II

is high and the integral term is not on the limit. Thus, during the acceleration mode, that is, when the speed error is above the error limit, ΔN^L, the relationship may be written as

$$\Delta N^L - K_N \dot{N}_e = 0$$

Solving for the rotor acceleration yields

$$\dot{N}_e = \frac{\Delta N^L}{K_N}$$

Consequently, unless otherwise limited by the

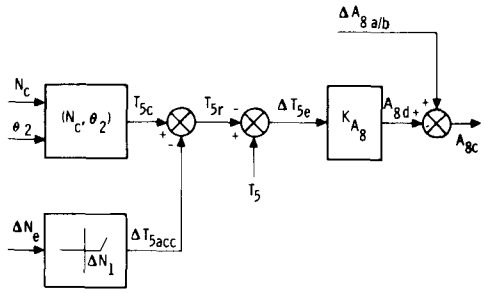

Fig.17 Turbine discharge temperature control loop

surge or overtemperature limit, the rotor acceleration is shown to be dependent on control parameters only, and therefore is a constant value regardless of engine speed and inlet conditions. The desired limit on rotor acceleration is set by the selection of the error limit, ΔN^L, which may be varied as a function of inlet condition.

Another advantage of this mode over Control Mode I is the reduction in overshoot. Reduction in the integral term commences at the time the speed error, ΔN_e, drops below the error limit, while in the previous system reduction in the integral term commences as the speed error goes through zero.

Test Results. The response of some of the system parameters to rapid acceleration demand, from 51 to 88 percent military speed, is shown in Fig.16. In general, the system performance is shown to be satisfactory. No overshoots during large transients were observed and limit cycles during the steady-state operation were not noticed.

Afterburner Operation

The DIGATEC concept was also applied to a

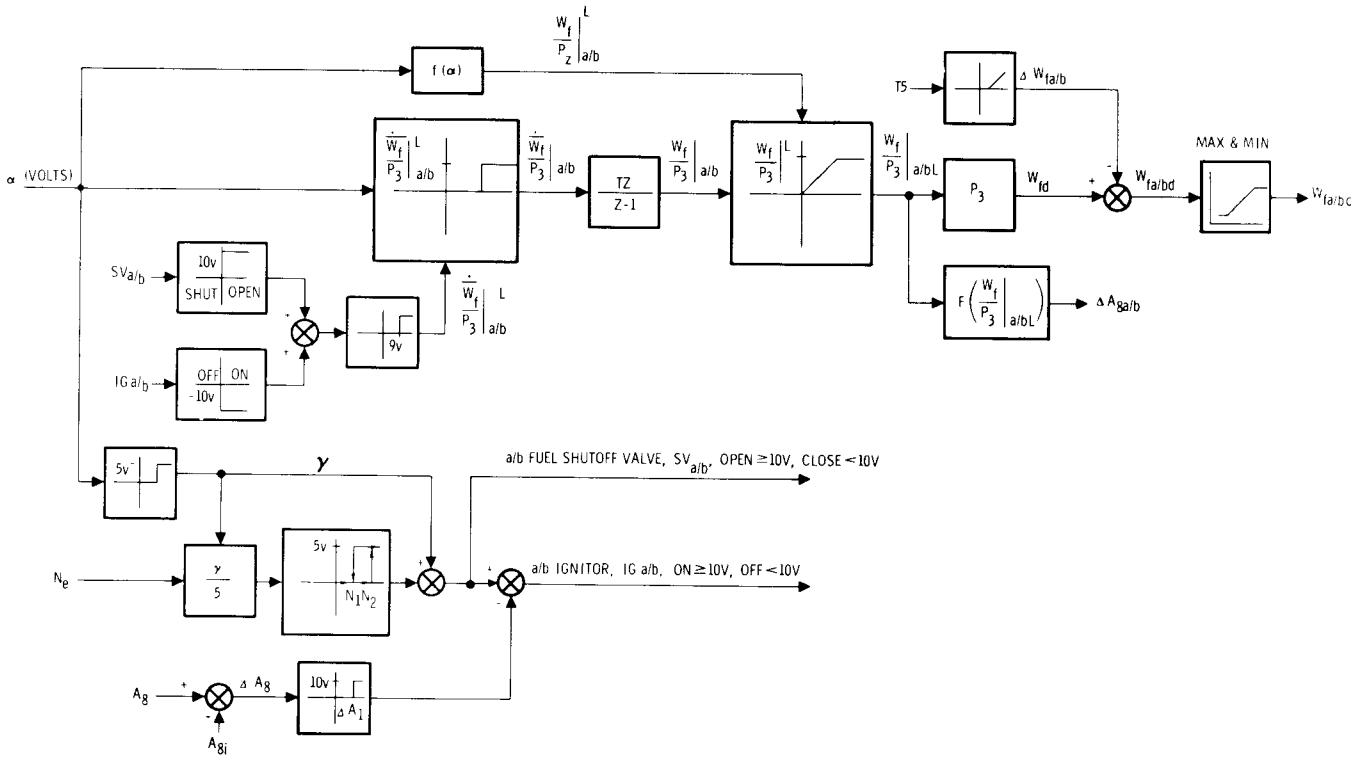

Fig.18 Afterburner fuel metering system

J85-5 afterburning engine. Automatic control of this engine from the Start Mode to maximum afterburner operation was demonstrated both in simulation and test phases. The closed loop speed control was similar to that described under Control Mode I with a modified exhaust nozzle area control.

Control Concept Description.

Turbine Discharge Temperature Control. A block diagram of this control loop is shown in Fig.17. Temperature control is accomplished through modulation of the exhaust nozzle area. The speed demand, which is a function of power lever position, and compressor inlet temperature establish the turbine discharge temperature demand T_{5C}. This demand is trimmed by $\Delta T_{5_{acc}}$ during rapid acceleration to yield T_{5R}, the reference temperature. The difference between the reference and actual temperature, ΔT_{5_e}, is calculated and the resulting temperature error is multiplied by a gain to yield the exhaust area demand, A_{8d}. The actual exhaust area command, A_{8c}, is the sum of the demand, A_{8d} and $\Delta A_{8\ a/b}$, the afterburner operating point exhaust nozzle area bias.

Since the steady-state temperature demand is essentially a function of the power lever position, the effect of actual rotor speed variation on this reference is eliminated. The result is a control loop more stable than that where a temperature reference is established by the actual speed. The major problem associated with the use of the power lever position to set the temperature reference, as pointed out earlier, is that the temperature tends to approach the requested level immediately upon the occurrence of a throttle burst which may result in compressor surge. This problem is avoided by the addition of the acceleration temperature reference reset path. During a large transient, the desired steady-state temperature is biased downward, the result being decreased rotor acceleration time and greater surge margin.

Afterburner Fuel System. A block diagram of the afterburner start and shutdown sequence of events and the fuel metering system is shown in Fig.18. In brief, two conditions must be met prior to the initiation of the afterburner operation mode. The power lever must be in the afterburner region and the speed above N_2. Hysteresis in the speed path is provided to prevent exit from the afterburner mode due to speed roll back following afterburner ignition.

Upon entering the afterburner mode, discretes are issued to open the shutoff valve and energize the ignitor. The afterburner fuel metering valve is then commanded to minimum fuel flow. Upon indication of afterburner ignition, several events take place: First, the ignitor is de-energized; second, the computer ramps the desired ratio of afterburner fuel flow to compressor discharge pressure at a constant rate, the maximum value of which is limited by the position of the

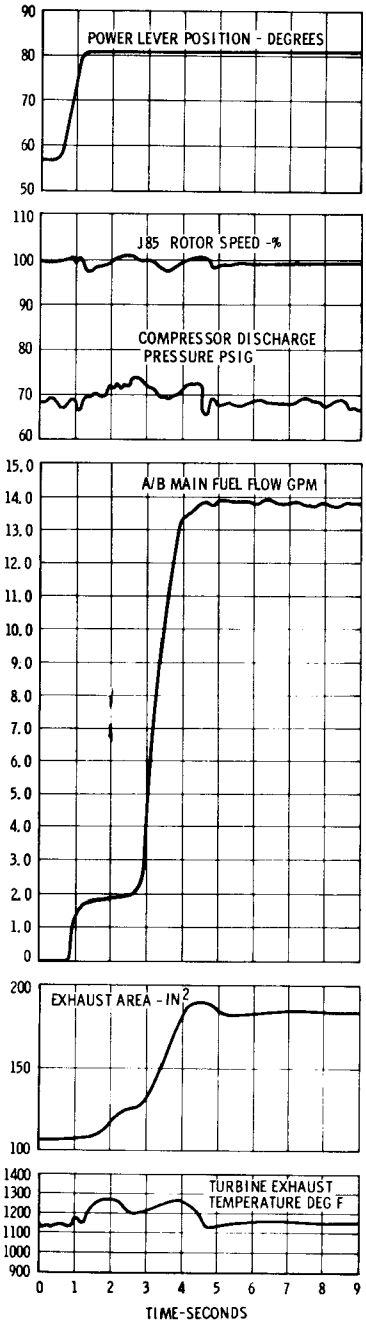

Fig.19 Response of critical engine parameters to advance of power lever and afterburner region

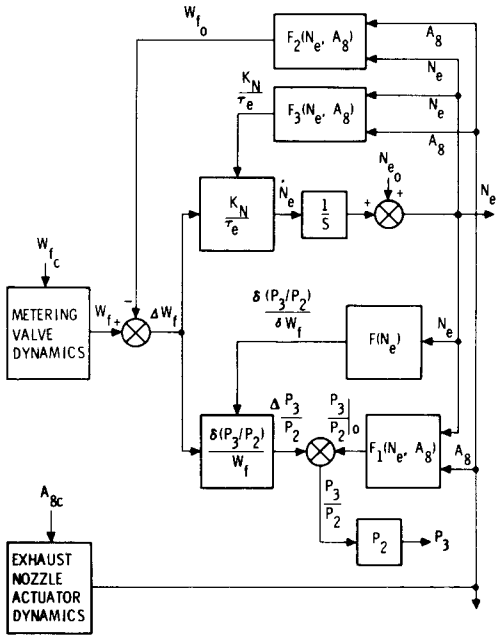

Fig.20 Simplified block diagram of analog computer simulation of the engine

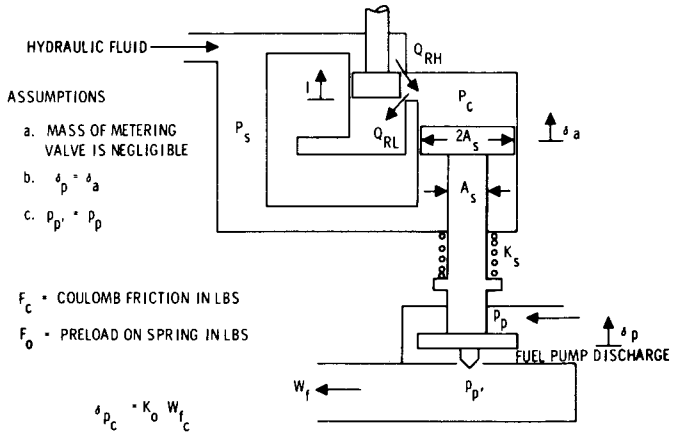

Fig.21 Fuel metering valve

power lever; and third, a bias on exhaust nozzle area command, $\Delta A_{8\ a/b}$, is generated. This parameter consists of a positive constant plus a term proportional to the ratio of afterburner fuel flow to compressor discharge pressure, $W_f/P_3|_{a/b\ L}$. The purpose of the constant term in the bias is to prevent an excessive speed transient due to loading variation on the compressor upon initiation or termination of afterburner operation. In general, this bias tends to reduce the temperature transient during rapid throttle change in the afterburner zone.

The limited W_f/P_3 is multiplied by the sensed compressor discharge pressure to yield the afterburner fuel flow demand, W'_{fd}. Overtemperature trim, $\Delta W_f|_{a/b}$, is applied to modify the demand, the purpose of which is to prevent excessive temperature due to slow response or failure of the exhaust nozzle actuator. The afterburner fuel flow is limited again just prior to issuance of the command to the metering valve.

The selection of the rate at which the ratio of afterburner fuel flow to compressor discharge pressure is increased is based on the maximum

available rate of the exhaust area actuator. Thus, the operator of the engine need not worry about how rapid he may advance the power lever in the afterburner region.

As far as the control logic is concerned, afterburner ignition has taken place if the exhaust nozzle area increases by a positive ΔA_1 from the instant the afterburner operating mode is initiated. This requires that the value of the exhaust nozzle area actuator position be picked up and stored at the time the afterburner ignition is issued for comparison with the instantaneous value of the exhaust nozzle area actuator position.

Exit from the afterburner mode is accomplished by retarding the power lever to a position below the afterburner operating region. Emergency shutdown of the main combustor fuel flow also acts to shut down the afterburner fuel flow.

Test Results of Afterburner Control. Fig.19 depicts the results of the afterburner control operation during a lightoff and max a/b demand. The data show the effects of the fuel scheduling after lightoff has been detected. Also shown are the effects on compressor discharge pressure of the action of the accommodation scheme during the lightoff period. The disturbance is a total of 4 psi or $\pm$ 3 percent. Nozzle area modulation and its effect on exhaust gas temperature are also indicated. The turbine discharge temperature rise following initiation of the afterburner was not high enough to trim the afterburner fuel flow.

APPENDIX 1

Equations for Simulation

During the simulation study, the engine was mechanized on an analog computer following the block diagram of Fig.20. The functions in the block diagram are defined by the relationships tabulated in Table 1. These relationships were derived by curve fit techniques from the engine maps.

Table 2 tabulates the relationships used for the fuel metering valve pictured schematically in Fig.21. Also given are the dynamic approximations used for the exhaust nozzle actuator.

Table 1 Tabulation of Analog Simulation

$$\dot{N}_e = \frac{K_n}{\tau_e}(W_f - W_{f_o}) \frac{rpm}{sec}$$

$$W_{f_o} = b_1 + a_1 (N_e - 7000)^2 \text{ PPH}$$

$$a_1 = 18.05 \times 10^{-6} - 3.810 \times 10^{-8} A_8 \frac{PPH}{(RPM)^2}$$

$$b_1 = 729 - 1.36 A_8 \text{ PPH}$$

$$\frac{K_N}{\tau_e} = b_2 + a_2 (N_e - 10{,}313)^2 \frac{RPM/SEC}{PPH}$$

$$a_2 = 0.766 \times 10^{-7} + 0.00716 \times 10^{-7} A_8 \frac{RPM/SEC}{PPH}/(RPM)^2$$

$$b_2 = 1.514 + 0.0252 A_8 \frac{RPM/SEC}{PPH}$$

$$\frac{P_3}{P_2} = \left.\frac{P_3}{P_2}\right|_0 + \frac{\partial(P_3/P_2)}{\partial W_f}(W_f - W_{f_o}) \frac{psi}{psi}$$

$$\frac{\partial(P_3/P_2)}{\partial W_f} = 0.000131 + 2.630 \times 10^{-8} N_e \frac{psi/psi}{PPH}$$

$$\left.\frac{P_3}{P_2}\right|_i = b_3 + a_3 (N_e - 7000)^2 \frac{psi}{psi}$$

$$a_3 = 5.27 \times 10^{-8} - 8.21 \times 10^{-11} A_8 \frac{psi/psi}{(RPM)^2}$$

$$b_3 = 1.634 - 1.610 \times 10^{-3} A_8 \text{ psi/psi}$$

$$P_3 = \frac{P_3}{P_2} \times P_2 \text{ psi}$$

Table 2 Relationship for Fuel Metering Valve

1.0 Metering Valve Equations

a. Hydraulic Valve Dynamics

$$I = \frac{K_e \omega_V^2}{(S + \omega_V)^2} (\delta_{p_c} - \delta_p)$$

$|I| \leq I_{Limit} = 8$ ma

$K_e = 200$ ma/in.

$\omega_V = 550$ rad/sec

b. Hydraulic Actuator Flow

$$Q_{RH} = -K_V I \sqrt{P_s - P_c} \qquad -I \geq 0$$

$$Q_{RL} = K_V I \sqrt{P_c} \qquad I > 0$$

$$Q_R = Q_{RL} - Q_{RH}$$

$$K_V = 0.0374 \ \frac{in^3}{sec\text{-}ma\sqrt{psi}}$$

$P_s = 900$ psia

c. Hydraulic Actuator Rate

$$\dot{\delta}_p = \frac{Q_R}{2A_s}$$

$2A_s = 1.57$ in^2

d. Control Pressure

$$P_p A_s + P_s A_s = P_c (2A_s) + F_o + K_s \delta_p + F_c$$

$$\therefore P_c = \frac{P_p}{2} + \frac{P_s}{2} - \frac{F_o}{2A_s} - \frac{K_s}{2A_s} \delta_p - \frac{F_c}{2A_s} \frac{\dot{\delta}_p}{|\dot{\delta}_p|}$$

or

$$P_c = \frac{P_p}{2} - 191\, \delta_p - 31.8 \frac{\dot{\delta}_p}{|\dot{\delta}_p|} + 434 \text{ psi}$$

e. Fuel Pump Discharge Pressure

$$P_p = 263 + 0.1228\, W_f + P_3 \text{ psi}$$

f. Engine Fuel Flow

$$W_f = \frac{K_c \omega_c}{S + \omega_c} \delta_p$$

$K_c = 10{,}000$ PPH/in.

$\omega_c = 50$ rad/sec

2.0 Exhaust Nozzle Area Actuators

$$A_8 = A_{8_{min}} + \frac{K_a \omega_a}{S + \omega_a} A_{8_c}$$

$K_a = 10$ in^2/volt

$\omega_a = 20$ rad/sec